Disruption of the Cereblon Gene Enhances Hepatic AMPK Activity and Prevents High-Fat Diet–Induced Obesity and Insulin Resistance in Mice

Kwang Min Lee,[1] Seung-Joo Yang,[1] Yong Deuk Kim,[2] Yoo Duk Choi,[3] Jong Hee Nam,[3] Cheol Soo Choi,[4,5] Hueng-Sik Choi,[2] and Chul-Seung Park[1]

A nonsense mutation in cereblon (*CRBN*) causes a mild type of mental retardation in humans. An earlier study showed that CRBN negatively regulates the functional activity of AMP-activated protein kinase (AMPK) in vitro by binding directly to the α_1-subunit of the AMPK complex. However, the in vivo role of *CRBN* was not studied. For elucidation of the physiological functions of *Crbn*, a mouse strain was generated in which the *Crbn* gene was deleted throughout the whole body. In *Crbn*-deficient mice fed a normal diet, AMPK in the liver showed hyperphosphorylation, which indicated the constitutive activation of AMPK. Since *Crbn*-deficient mice showed significantly less weight gain when fed a high-fat diet and their insulin sensitivity was considerably improved, the functions of *Crbn* in the liver were primarily investigated. These results provide the first in vivo evidence that Crbn is a negative modulator of AMPK, which suggests that *Crbn* may be a potential target for metabolic disorders of the liver. *Diabetes* 62:1855–1864, 2013

Initially, cereblon (*CRBN*) was identified as a target gene for a mild type of mental retardation in humans (1) and was subsequently characterized in several different functional contexts. CRBN interacts directly with large-conductance calcium-activated potassium channels and regulates their surface expression (2). Later, CRBN was identified as a primary target for thalidomide-induced teratogenicity and as a substrate receptor for the E3 ligase complex (3). More recently, we reported that CRBN interacts directly with the α_1-subunit of AMP-activated protein kinase (AMPK) and inhibits activation of the enzyme in vitro (4).

AMPK is a metabolic master switch in response to variations in cellular energy homeostasis (5). The activity of AMPK can be modulated by the phosphorylation of a threonine at position 172 (Thr172) in the α-subunit by upstream kinases such as LKB1 (6). AMPK inactivates acetyl-CoA carboxylase (ACC) via direct protein phosphorylation and suppresses expression of lipogenic genes, including fatty acid synthase (FAS), thereby inhibiting fatty acid synthesis (7,8). AMPK is implicated in the regulation of hepatic glucose and lipid metabolism, thereby affecting the energy status of the whole body (7,9). Moreover, AMPK was identified as a major pharmacological target protein for the treatment of metabolic diseases. For example, experimental animal models of type 2 diabetes and obesity show that activation of AMPK by metformin or 5-aminoimidazole-4-carboxamide ribonucleoside reduces blood glucose levels and improves lipid metabolism (10–12).

Our recent study found that CRBN interacted directly with the AMPK α_1-subunit both in cultured cell lines and in vitro, and the binding sites within the two proteins were localized (4). The levels of the AMPK γ-subunit and CRBN in the AMPK complex varied in a reciprocal manner; i.e., a higher CRBN content corresponded to lower γ-subunit content. AMPK activation was reduced as its γ-subunit content was decreased by CRBN. Thus, it was proposed that CRBN may act as a negative regulator of AMPK in vivo (4). The aims of the current study were to test this hypothesis and to understand the physiological role(s) of *CRBN* by generating *Crbn* knockout (KO) mice. The results showed that AMPK activity was activated constitutively in *Crbn* KO mice under normal conditions and that *Crbn* KO mice fed a long-term high-fat diet (HFD) showed a marked improvement in their metabolic status.

RESEARCH DESIGN AND METHODS

Generation of *Crbn* KO mice. For generation of *Crbn* KO mice, heterozygous F1 animals were provided by the knockout mouse service (Macrogen, Seoul, Korea). The targeting vector used to delete a segment containing exon 1 of the *Crbn* gene (1.1 kb) was constructed using a 5′ short arm fragment (2.6 kb) and a 3′ long arm fragment (7.3 kb), which were ligated into the pOsdupdel vector. The targeting vector was constructed by replacing the 1.1-kb genomic segment with the neomycin cassette. Heterozygous F1 animals were backcrossed with C57BL/6N mice over at least 10 generations before this study. Heterozygous males and females were then bred to produce *Crbn* KO mice. The genotypes of the WT and *Crbn* KO mice were determined by RT-PCR using tail genomic DNA and primers specific for wild-type (WT) or *Crbn* KO alleles (P1, P2, and P3 in Fig. 1*A*).

Experimental animals. Mice were maintained on a standard chow diet and water ad libitum in pathogen-free conditions and housed in a room with a 12-h light-dark cycle. For induction of obesity and insulin-resistant phenotypes, male mice (5 weeks old; *n* = 12–13 per group) were fed an HFD (Research Diet D12492) for 14 weeks while being housed separately. Body weight and food intake were recorded throughout the experiments. Food intake was assessed by determining the difference in food weight during a 7-day period. All experiments were approved by the Gwangju Institute of Science and Technology Animal Care and Use Committee.

Insulin sensitivity. Glucose tolerance tests were performed by intraperitoneally injecting mice with D-glucose (Sigma) at a dose of 2 g/kg body

FIG. 1. Generation of *Crbn* KO mice. *A*: The vector construct used to generate *Crbn* KO (*Crbn*^{−/−}) mice. The genotyping primers are indicated as P1, P2, and P3. *B*: Genotypes of the WT (*Crbn*^{+/+}), heterozygous KO (*Crbn*^{+/−}), and homozygous KO (*Crbn*^{−/−}) mice were determined by RT-PCR using tail genomic DNA. *C*: Protein extracts from liver, SKM, or WAT of *Crbn*^{+/+} and *Crbn*^{−/−} mice showing the levels of endogenous Crbn protein as determined by Western blotting. β-Actin was used as the loading control. (*n* = 4 per group.) *D*: Western blots of endogenous AMPK-α, P–AMPK-α, ACC, and P-ACC in *Crbn*^{+/+}, *Crbn*^{+/−}, and *Crbn*^{−/−} primary MEFs. Glyceraldehyde-3-phosphate dehydrogenase (GAPDH) was used as the loading control. The results shown are representative of four independent experiments (*E* and *F*). Relative band intensities as determined by densitometric analysis of the blots in *D*. Error bars represent the SEM.

wt after a 16-h fast. Insulin tolerance tests were performed intraperitoneally by injecting human insulin (Sigma) at a dose of 0.75 units/kg body wt after a 4-h fast. Blood samples were collected via the tail vein, and plasma glucose levels were measured using a glucometer (Roche Diagnostics).

Histological analysis of the liver. At the end of the 14-week period, mice were killed and the livers fixed in 10% formalin and embedded in paraffin. Paraffin sections (5 μm) were then subjected to hematoxylin and eosin (H&E) staining. Cryosections were stained using Oil Red O and counterstained with hematoxylin to visualize the lipid droplets.

Quantitative real-time PCR analysis. Total RNA was isolated from liver tissues of the indicated mice with TRIzol reagent (Invitrogen) according to the manufacturer's protocol. Expression was normalized against the levels of β-actin mRNA. The sequences of the primers used in the PCR analyses are described in Supplementary Table 1.

Statistical analysis. All values were expressed as means ± SEM. Significant differences between groups were determined using two-tailed unpaired Student *t* tests, and multiple comparisons were performed using one-way ANOVA

or two-way repeated-measures ANOVA. Differences with *P* < 0.05 were considered statistically significant and are shown in the Figure legends.

RESULTS

Generation of *Crbn* KO mice and genotyping. *Crbn* KO mice were generated to elucidate the in vivo function of *Crbn*. (Fig. 1*A*). PCR analysis of genomic DNA from the tails of *Crbn* KO mice confirmed the loss of the WT gene and the presence of the targeting vector (Fig. 1*B*). Crbn protein was not detected in the liver, skeletal muscle (SKM), or white adipose tissue (WAT) (Fig. 1*C*), and all other tissues were tested by Western blot analysis. The daily body weight of both male and female KO mice fed a normal diet from weaning to 12 weeks of age was comparable with that of WT mice (Supplementary Fig. 1*A*).

Our previous study showed that CRBN inhibits the activation of AMPK in vitro by interacting directly with the α_1-subunit of AMPK (AMPK-α_1) (4); therefore, the current study examined whether *Crbn* deficiency affected AMPK activation (Fig. 1*D*). First, the phosphorylation of AMPK Thr172 was measured in primary mouse embryonic fibroblasts (MEFs). The amount of phosphorylated (P-)AMPK-α increased in $Crbn^{+/-}$ and $Crbn^{-/-}$ MEFs (Fig. 1*E*). ACC is inactivated by phosphorylation of serine 79 after AMPK activation; therefore, we next measured the levels of P-ACC. Increases in P-AMPK were accompanied by higher levels of P-ACC in $Crbn^{+/-}$ and $Crbn^{-/-}$ MEFs compared with $Crbn^{+/+}$ MEFs (Fig. 1*F*). It was shown previously that the binding of exogenous CRBN to AMPK decreases the amount of γ-subunits in the AMPK complex (4); therefore, the effects of *Crbn* KO on the AMPK complex were tested by immunoprecipitating the endogenous AMPK complex from MEFs (Supplementary Fig. 1*C–F*). The intensity of the AMPK β-band did not change greatly (Supplementary Fig. 1*D*); however, the intensity of the γ_1-subunit band was significantly higher in both $Crbn^{+/-}$ and $Crbn^{-/-}$ MEFs compared with $Crbn^{+/+}$ (Supplementary Fig. 1*E*). These results support the hypothesis that CRBN suppresses AMPK activation by reducing the affinity of the γ_1-subunit for the AMPK complex (4).

AMPK is activated in *Crbn* KO mice. For testing of whether *Crbn* deficiency affected the function of AMPK in vivo, the enzymatic activity of AMPK was assessed in the mouse liver by determining its phosphorylation state. AMPK phosphorylation was 8.2-fold higher in *Crbn* KO mice than in WT (Fig. 2*A* and Supplementary Fig. 2*A*).

Subsequently, the effects of *Crbn* KO were investigated under conditions known to activate endogenous AMPK (13,14). The level of AMPK phosphorylation increased in a time-dependent manner in both WT and *Crbn* KO mice after injection of metformin; however, the level of P–AMPK-α was higher in *Crbn* KO mice than that in WT (Fig. 2*B* and Supplementary Fig. 2*B*). Similar results were obtained with primary MEFs cultured under serum-deprived conditions. (Supplementary Fig. 2*C* and *D*). Overall, these results suggest that AMPK is hyperactivated in the absence of *Crbn* in vivo, which further indicates that Crbn acts as an endogenous negative regulator of AMPK.

Crbn deficiency has a protective effect against HFD-induced obesity. For elucidation of the physiological role(s) of *Crbn* in vivo, both WT and *Crbn* KO mice were fed either a normal chow diet or an HFD (Fig. 3*A* and *B*). The HFD-induced weight increase was slower and the level of weight gain was much less for *Crbn* KO mice than for the WT. The body weight of WT mice fed the HFD was significantly higher than that of mice fed the chow diet at 2 weeks, whereas the *Crbn* KO mice were significantly heavier at 7 weeks (Fig. 3*E*). The difference in the HFD-induced weight gain of WT and *Crbn* KO mice was not attributable to their food consumption (Fig. 3*F*). The initial average weight of *Crbn* KO mice was also not significantly different from that of WT mice (Fig. 3*E* and Supplementary Table 2).

Necropsies were performed on both WT and *Crbn* KO mice, which showed that *Crbn* KO mice fed the HFD had a lower epididymal fat mass than WT (Fig. 3*C* and *D*). After 14 weeks on the HFD, the average epididymal fat mass of
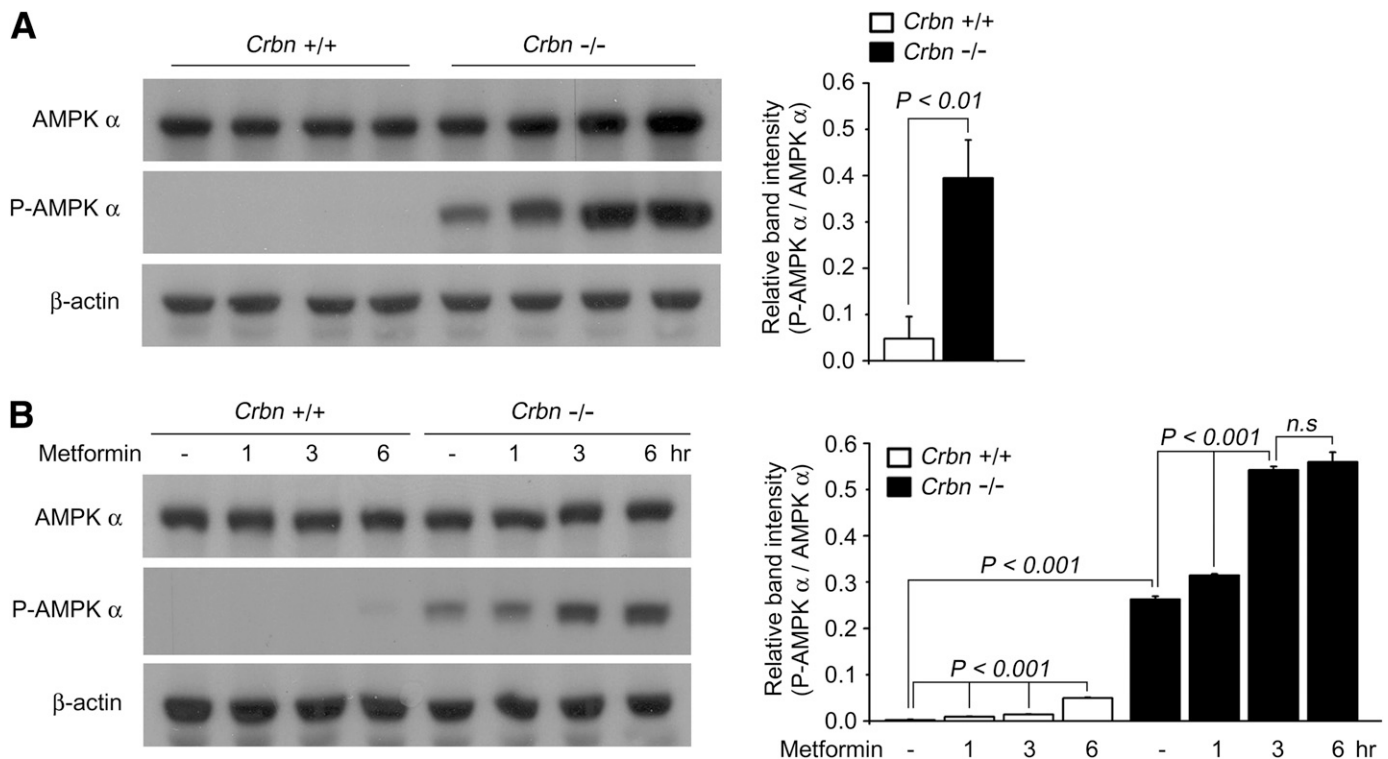
FIG. 2. Increased AMPK activation in the $Crbn^{-/-}$ liver. *A*: Proteins extracted from the livers of $Crbn^{+/+}$ and $Crbn^{-/-}$ mice were separated by SDS-PAGE and immunoblotted with anti–AMPK-α, anti–P–AMPK-α, and anti–β-actin antibodies. Nine-week-old male mice were used ($n = 9$ per group). β-Actin was used to confirm equal protein loading. Error bars represent the SEM. *B*: Liver lysates were prepared and subjected to Western blot analysis with anti–AMPK-α, anti–P–AMPK-α, and anti–β-actin antibodies. The numbers represent the time after intraperitoneal injection of metformin at a dose of 150 mg/kg body wt. Nine-week-old male mice were used ($n = 5$ per group). β-Actin was used to confirm equal protein loading. Error bars represent the SEM.
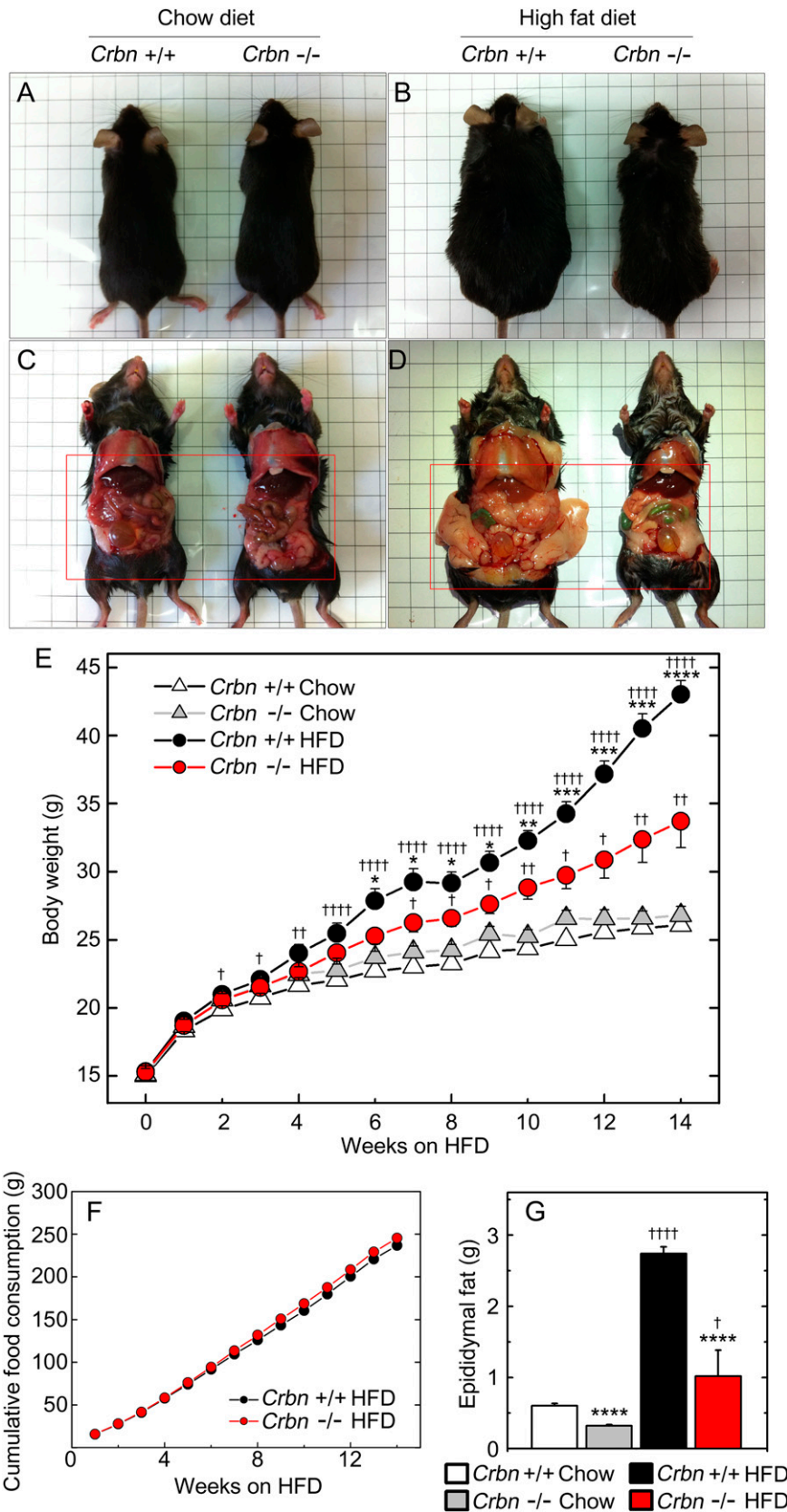
FIG. 3. *Crbn* deficiency prevented HFD-induced obesity. *A–D*: Representative images of mice fed a normal chow diet or an HFD at the end of the 14-week experimental period. *E*: Body weight changes in WT and *Crbn* knockout mice fed a normal chow diet or an HFD were monitored weekly during the 14-week experimental period. *F*: Cumulative food consumption of WT and *Crbn* KO mice fed an HFD for 14 weeks. *G*: Epididymal fat mass of mice at the end of the 14-week experiment. Error bars represent the SEM (n = 12–13 per group). *Statistical differences (*$P < 0.05$, **$P < 0.01$, ***$P < 0.005$, ****$P < 0.001$) vs. WT mice fed the same diet. †Statistical differences (†$P < 0.05$, ††$P < 0.01$, †††$P < 0.005$, ††††$P < 0.001$) vs. mice with the same genotype that were fed the normal chow diet.

WT mice was 2.7-fold higher than that of *Crbn* KO. *Crbn* KO mice fed with a normal chow diet had lower epididymal fat masses than WT (Fig. 3*G*). These observations suggest that mice lacking Crbn experienced greater protection from body fat accumulation and obesity caused by high fat intake.

Crbn KO mice are resistant to diet-induced fatty liver. The effects of HFD on the morphology and lipid content of the liver in *Crbn* KO mice were tested next. A comparison of the livers from HFD-fed WT and *Crbn* KO mice showed that WT livers were much larger, heavier, and paler than those of *Crbn* KO mice (Fig. 3*D* and Fig. 4*A*). The hepatic triglyceride (TG) content was significantly lower in HFD-fed *Crbn* KO mice than in the WT. The TG content was also lower in *Crbn* KO mice fed the normal chow diet than in WT (Fig. 4*B*). Hepatic cholesterol levels were also higher in both WT and Crbn KO mice fed an HFD (Fig. 4*C*).

In agreement with these results, H&E staining of liver sections showed that the livers of HFD-fed WT mice contained unstained lipid inclusions, which were less abundant in the livers of HFD-fed *Crbn* KO mice (Figs. 4*D–G*).

Oil Red O staining of lipids further confirmed the massive accumulation of neutral lipids in the livers of WT mice fed an HFD, which is a hallmark of fatty liver, but not in the livers of *Crbn* KO fed an HFD (Figs. 4*H–K*). Thus, *Crbn* deficiency prevented the accumulation of fats in the epididymal tissues and liver, which made the livers more resistant to fatty liver, which is normally caused by high fat intake.

Crbn KO mice fed an HFD show improved glucose homeostasis and insulin sensitivity. *Crbn* KO mice were largely protected from HFD-induced obesity and fatty liver; therefore, we next investigated their metabolic parameters. When fed an HFD, WT mice showed significantly higher levels of serum glucose, insulin, and leptin than mice fed normal chow (Fig. 5*A–C*), which suggests impaired insulin sensitivity. However, the serum levels of glucose, insulin, and leptin were significantly lower in HFD-fed *Crbn* KO mice. Other plasma metabolic parameters were also measured in both WT and *Crbn* KO mice fed normal chow or the HFD (Supplementary Fig. 3). Under both diet conditions, WT and Crbn KO mice showed similar serum levels of TG, cholesterol, resistin, adiponectin,
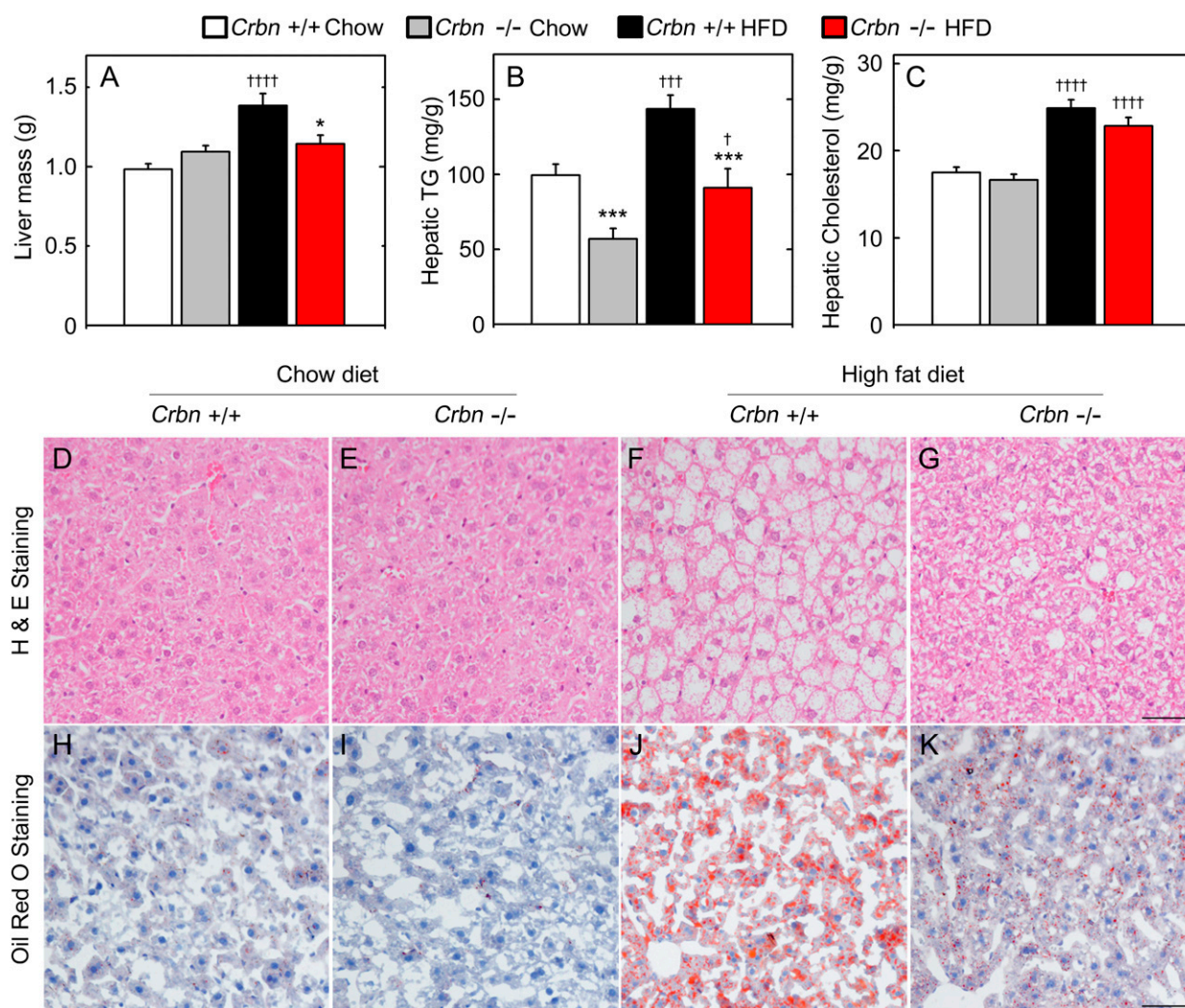
FIG. 4. *Crbn* deficiency in the mouse liver prevented fatty liver. *A*: Liver mass of WT and *Crbn* KO mice fed a normal chow diet or HFD at the end of the 14-week experimental period. *B*: Hepatic TG levels. *C*: Hepatic cholesterol levels. *D–G*: Liver sections of the indicated mice were stained with H&E. Scale bar = 50 μm. *H–K*: Lipids in the liver section of the indicated mice were stained with Oil Red O. Scale bar = 50 μm. Error bars represent the SEM (n = 9–10 per group). *Statistical differences (*$P < 0.05$, **$P < 0.01$, ***$P < 0.005$, ****$P < 0.001$) vs. WT mice fed the same diet. †Statistical differences (†$P < 0.05$, ††$P < 0.01$, †††$P < 0.005$, ††††$P < 0.001$) vs. mice with the same genotype that were fed the normal chow diet.
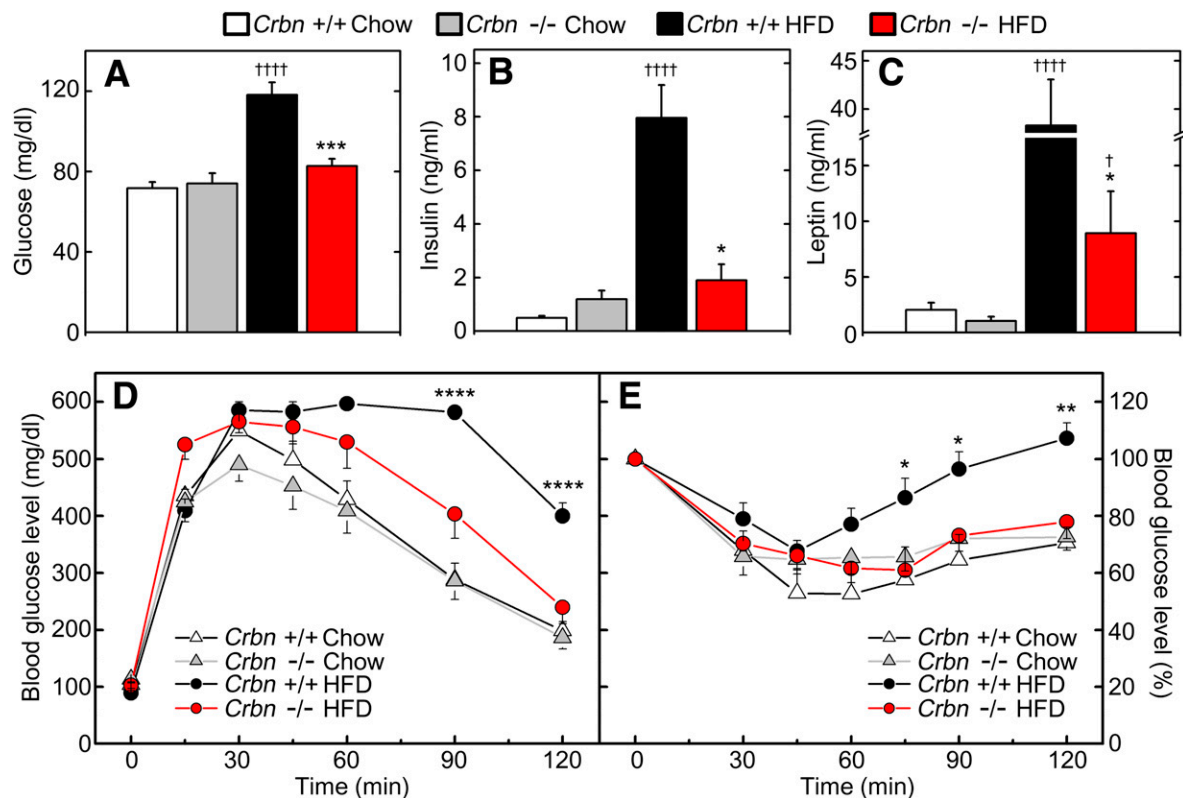
FIG. 5. Glucose homeostasis and insulin sensitivity in $Crbn^{-/-}$ mice under HFD conditions. Plasma glucose concentration (A), plasma insulin concentration (B), and plasma leptin concentration (C) in WT and $Crbn$ KO mice fed a normal chow diet or an HFD at the end of the 14-week experimental period. D: Intraperitoneal glucose tolerance test. F: Intraperitoneal insulin tolerance test. Error bars represent the SEM (n = 9–10 per group). *Statistical differences (*$P < 0.05$, **$P < 0.01$, ***$P < 0.005$, ****$P < 0.001$) vs. WT mice fed the same diet. †Statistical differences (†$P < 0.05$, ††$P < 0.01$, †††$P < 0.005$, ††††$P < 0.001$) vs. mice with the same genotype that were fed the normal chow diet.

tumor necrosis factor-α, MCP-1, and plasminogen activator inhibitor-1. By contrast, the serum nonesterified FFA levels of $Crbn$ KO mice fed an HFD were lower than those in the WT (Supplementary Fig. 3C), which agrees with a previous report showing that type 2 diabetic patients with a fatty liver are substantially more insulin resistant and have higher levels of plasma FFA (15). Increased glucose tolerance and insulin sensitivity were also confirmed in HFD-fed $Crbn$ KO mice. (Fig. 5D and E). These results demonstrate that $Crbn$ deficiency may prevent glucose intolerance and insulin resistance, which are normally induced by a long-term HFD.

$Crbn$ deficiency alters lipid metabolism and glucose metabolism in the liver. For elucidation of the molecular basis of the phenotypic changes observed in $Crbn$ KO mice fed an HFD, expression profiling was performed for several metabolic enzymes. AMPK activation was also monitored. The level of P-AMPK was lower in mice fed an HFD (Fig. 6A), which is in agreement with previous studies (16,17). The total AMPK expression level was not different between WT and $Crbn$ KO mice fed a normal chow diet or an HFD, whereas P-AMPK was significantly higher in $Crbn$ KO mice fed an HFD than in WT mice fed an HFD (Fig. 6B). Furthermore, the ratio of P-ACC to total ACC was consistent with the level of AMPK-α activation (Fig. 6D). Despite the hyperphosphorylation of AMPK, the expression levels of the AMPK upstream kinases, liver kinase and Ca^{2+}/calmodulin-dependent protein kinase kinase β, were similar in $Crbn$ KO mice and WT mice (Supplementary Fig. 4), suggesting that these kinases may not be involved in AMPK activation in $Crbn$ KO mice.

There were no statistical differences in the expression of $SREBP1C$ or $ChREBP$ (Fig. 7A and B), a major regulator of lipogenesis (18,19) between the groups; however, the expression of $PPAR\gamma$, a lipogenic transcription factor (20,21), was significantly lower in $Crbn$ KO fed either a normal chow diet or an HFD compared with that in WT mice fed these diets (Fig. 7C). The expression of FAS, which is involved in fatty acid synthesis, and $DGAT2$, a rate-limiting enzyme that catalyzes the final step of TG synthesis (22,23), was reduced in $Crbn$ KO mice fed a normal chow diet or the HFD (Fig. 7D and E). These results are consistent with the finding that the level of hepatic TG was lower in $Crbn$ KO mice fed both the normal chow diet and the HFD compared with that in the WT mice (Fig. 4B). The expression levels of $ACC1$ and $SCD1$ mRNA were significantly lower in HFD-fed $Crbn$ KO mice than in HFD-fed WT (Fig. 7F and G). Expression of $G6Pase$, but not $PEPCK$, was significantly lower in $Crbn$ KO mice fed both the normal chow diet and the HFD than in WT (Fig. 7H and I). The expression of L-PK, which is a key enzyme involved in glycolysis, was significantly higher in WT mice fed the HFD; however, its upregulation was completely abrogated in $Crbn$ KO mice fed the HFD (Fig. 7L). This result is consistent with serum glucose levels (Fig. 5A) because L-PK gene transcription is positively regulated by glucose and insulin (24,25). The pattern of AMPK activation (Fig. 6A) is also consistent with the reciprocal pattern of mRNA expression for L-PK and $G6Pase$ (Fig. 7M and I); AMPK activation inhibits the expression of L-PK (25,26) and $G6Pase$ (27). Expression of $FGF21$ was 10.3-fold higher in WT mice fed an HFD than in
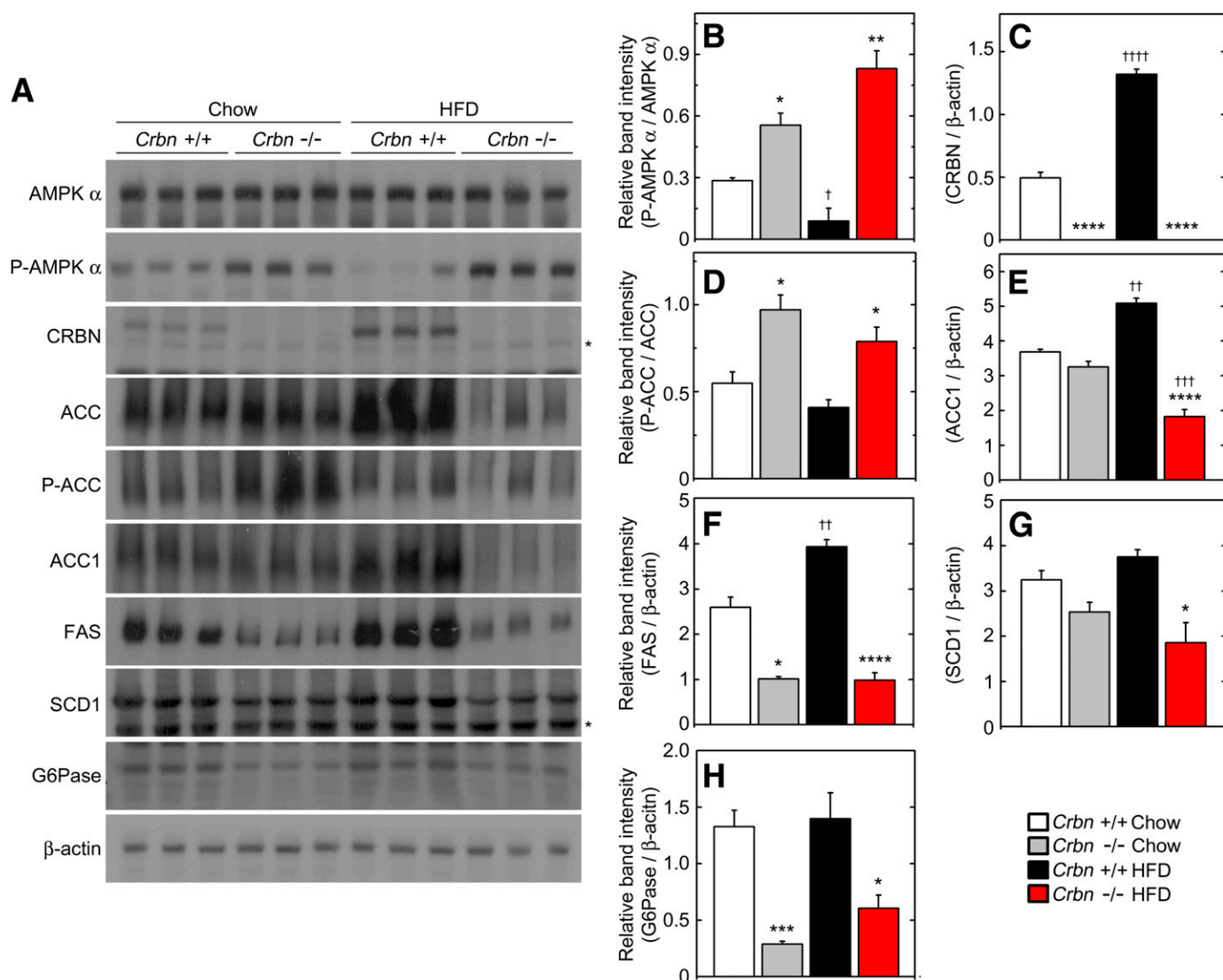
FIG. 6. *Crbn* KO mice fed an HFD showed AMPK activation and ACC inhibition in the liver. *A*: Western blotting analysis of AMPK-α, P–AMPK-α, Crbn, ACC, P-ACC, ACC1, FAS, SCD1, and G6Pase protein levels in liver tissue lysates. β-Actin was used as the loading control. *Nonspecific bands. *B*: The ratio of P–AMPK-α to AMPK-α. *C*: The ratio of Crbn to β-actin. *D*: The ratio of P-ACC to total ACC. *E*: The ratio of ACC1 to β-actin. *F*: The ratio of FAS to β-actin. *G*: The ratio of SCD1 to β-actin. *H*: The ratio of G6Pase to β-actin on the blot in *A*. Error bars represent the SEM ($n = 9$–10 per group). *Statistical differences (*$P < 0.05$, **$P < 0.01$, ***$P < 0.005$, ****$P < 0.001$) vs. WT mice fed the same diet. †Statistical differences (†$P < 0.05$, ††$P < 0.01$, †††$P < 0.005$, ††††$P < 0.001$) vs. mice with the same genotype that were fed the normal chow diet.

WT fed a normal chow diet (Fig. 7*J*), which is consistent with a previous report showing that obesity may be considered an FGF21-resistant state (28). However, *FGF21* expression was only 3.7-fold higher in Crbn KO mice fed an HFD than that in *Crbn* KO mice fed normal chow. The mRNA expression levels of *HMGCS*, which is involved in cholesterol biosynthesis, were 1.8-fold higher in HFD-fed WT mice compared with those in normal chow-fed WT mice (Fig. 7*K*). Unexpectedly, *HMGCS* expression was 1.7-fold higher in *Crbn* KO mice fed normal chow than in WT fed normal chow. The induction of *HMGCS* in *Crbn* KO mice fed a normal chow diet did not correlate with the observed phenotypes of the WT and *Crbn* KO mice. This may be due to compensatory gene induction to maintain hepatic homeostasis. There were no changes in the expression of *Dhcr24*, which is involved in cholesterol biosynthesis and *HSL*, which is involved in lipolysis (Fig. 7*L* and *N*). The protein expression patterns of ACC1, FAS, SCD1, G6Pase, and Crbn (Fig. 6*A*, *C*, and *E–H*) were consistent with the mRNA expression profiles shown in Fig. 7.

Expression of ACC1 was also increased in WT mice fed an HFD compared with those fed a normal chow diet (Fig. 6*E*). Overall, these results show that the disruption of *Crbn* affects the expression of many key metabolic genes. The expression of several lipogenic and gluconeogenic proteins, which are upregulated by HFD, was significantly lower in the livers of *Crbn* KO mice, which may be explained by the constitutive activation of AMPK (9,23,25–27).

DISCUSSION

Crbn is evolutionarily conserved between plants and animals and is expressed widely in various mammalian tissues. For validation of the in vivo function of *Crbn* as a novel regulator of AMPK, *Crbn* KO mice were established. The *Crbn* KO mice were viable, with no apparent defects in gross morphology or basic behavior.

As suggested by a previous knockdown study of endogenous CRBN in cultured cell lines (4), endogenous AMPK was constitutively hyperactivated in *Crbn* KO mice
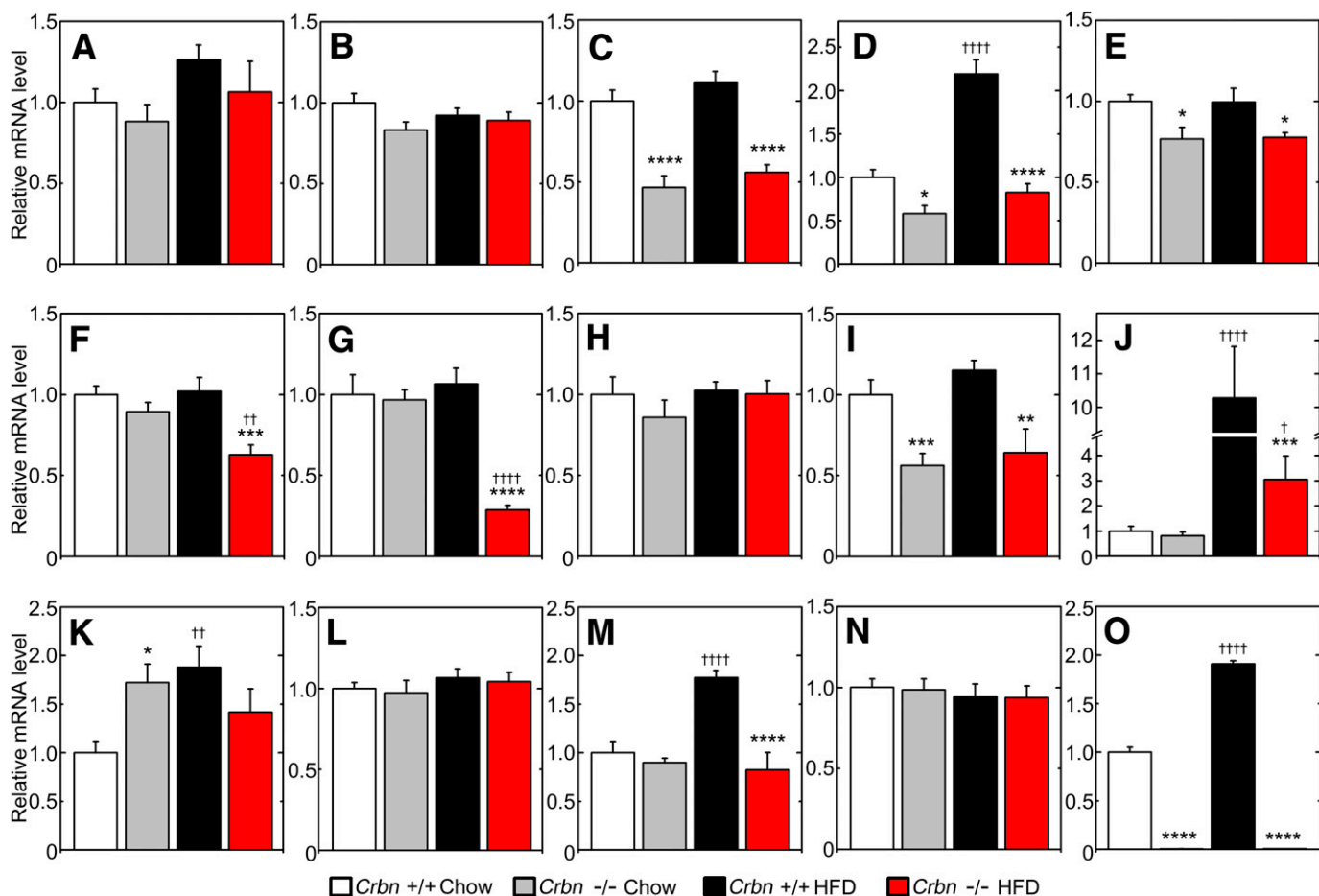
FIG. 7. Deletion of *Crbn* resulted in the defective expression of genes involved in hepatic glucose and lipid metabolism. *A–O*: Total RNA was isolated from the liver tissues of the indicated mice and subjected to quantitative real-time PCR analysis to determine the expression of *SREBP1C* (*A*), *ChREBP* (*B*), *PPARγ* (*C*), *FAS* (*D*), *DGAT2* (*E*), *ACC1* (*F*), *SCD1* (*G*), *PEPCK* (*H*), *G6Pase* (*I*), *FGF21* (*J*), *HMGCS* (*K*), *Dhcr24* (*L*), *L-PK* (*M*), *HSL* (*N*), and *Crbn* (*O*). Expression was normalized against β-actin mRNA levels. Fold changes in the mRNA levels relative to WT mice fed a normal chow diet, which were set arbitrarily at 1.0, are shown. Error bars represent the SEM (*n* = 9–10 per group). *Statistical differences (*$P <$ 0.05, **$P <$ 0.01, ***$P <$ 0.005, ****$P <$ 0.001) vs. WT mice fed the same diet. †Statistical differences (†$P <$ 0.05, ††$P <$ 0.01, †††$P <$ 0.005, ††††$P <$ 0.001) vs. mice with the same genotype that were fed the normal chow diet.

under normal conditions in all tissues tested; therefore, *Crbn* KO mice were fed an HFD before assessment of the effects of *Crbn* deficiency on several parameters: body weight, fatty liver, glucose homeostasis, insulin resistance, and metabolic parameters. In general, *Crbn* KO mice fed an HFD showed a significant improvement in their metabolic profiles compared with HFD-fed WT control mice. Also, *Crbn* KO mice showed no signs of metabolic syndrome, even after 14 weeks on an HFD. Fat accumulation within the epididymal tissue and liver was also markedly reduced in KO mice. Thus, it was hypothesized that hyperactivity of AMPK in *Crbn* KO mice was the major contributor to the overall improvement in lipid and glucose homeostasis and insulin sensitivity. It was intriguing that Crbn expression was significantly upregulated, whereas that of P-AMPK was correspondingly downregulated in the livers of WT mice on an HFD. This observation agreed with our previous prediction that Crbn might negatively regulate the functional activity of AMPK in vivo (4).

The current study focused on the effects of *Crbn* KO on the liver and hepatic metabolism because the liver plays a key role in controlling overall energy status, whereas AMPK coordinates changes in the hepatic enzymes involved in carbohydrate and lipid metabolism. Activation of

hepatic AMPK inhibits lipogenesis, cholesterol synthesis, and glucose production (7,8,29). The lower expression of lipogenic regulators, including *FAS*, *ACC1*, *SCD1*, *PPARγ*, and *DGAT2*, observed in HFD-fed *Crbn* KO mice suggests that inhibition of hepatic lipogenesis may contribute to lower levels of fat accumulation. The hepatic expression of *G6Pase* was lower in *Crbn* KO mice fed an HFD, suggesting lower levels of gluconeogenesis. Consistent with these findings, the glucose and insulin tolerance tests showed restoration of normal levels in *Crbn*-deficient mice fed an HFD. Infection with adenovirus encoding a dominant-negative AMPK mutant (Ad-DN-AMPK) increased the glucose output of primary *Crbn* KO hepatocytes in a dose-dependent manner in comparison with *Crbn* KO hepatocytes infected with Ad-GFP (Supplementary Fig. 5). Collectively, this suggests that the primary mechanism by which KO of *Crbn* reduces lipogenesis and gluconeogenesis in the liver operates, at least in part, by regulating AMPK and ACC activity via protein phosphorylation. Furthermore, the levels of Crbn protein and P-AMPK showed a strongly correlation in vivo because the levels of Crbn expression increased as P-AMPK expression decreased in WT mice fed an HFD.

There were several noticeable changes in the expression of key metabolic genes in *Crbn* KO mice fed a regular

chow diet, suggesting a physiological role for *Crbn* under normal conditions. For example, the expression of lipogenic genes, such as *FAS*, *PPARγ*, and *DGAT2* and a gluconeogenic gene, *G6Pase*, was significantly lower. In a good agreement with these findings, hepatic TG levels and the epididymal fat mass were lower in *Crbn* KO mice fed a regular diet than in WT fed a regular diet. However, morphological phenotypes, including body weight, liver weight, liver morphology, liver section, glucose tolerance, and insulin sensitivity, were similar in WT and *Crbn* KO mice before the HFD was started. Therefore, *Crbn* deficiency conferred greater resistance to a metabolic syndrome phenotype under severe pathophysiological conditions (such as a HFD) but not under normal physiological conditions.

In our previous report, AMPK-α_1 was identified as a CRBN-binding protein (4). Two isoforms of the AMPK-α, AMPK-α_1 and AMPK-α_2, are found in mammals (30). AMPK complexes containing each α-subunit isoform were equally represented in terms of total AMPK activity in the liver (26). The current study examined the interaction between AMPK-α_2 and Crbn. There was no difference in the binding affinity of Crbn for AMPK-α_1 or AMPK-α_2 (Supplementary Fig. 6). This was because the putative Crbn-binding site in AMPK-α_1 is within a region covering amino acids 394–422 (4), which is also highly conserved in AMPK-α_2 (within a region covering amino acids 388–417). These results suggested that Crbn can modulate cellular AMPK, irrespective of its subtype.

It is important to determine whether the *Crbn*-dependent inhibition of AMPK is also conserved in other organisms, especially humans. Our previous study showed that the activity of AMPK was inhibited by the expression of exogenous Crbn in human, rat, and mouse cell lines (4), so it is likely that the negative regulation of AMPK by CRBN also occurs in humans. Recently, *CRBN*, which is located in the 3p26–25 region in humans, was identified as a target gene for obesity and insulin. Several single nucleotide polymorphisms close to the *CRBN* gene are associated with central obesity and high blood pressure in humans and the mice (31), indicating the potential clinical relevance of CRBN in metabolic syndromes.

However, several important questions still need to be addressed. First, the regulation of *Crbn* gene expression is not understood. *Crbn* expression was upregulated in the long term by high fat intake (Fig. 6*O* and 7*C*). This observation implies that Crbn is induced by an HFD and that CRBN regulates AMPK activity via a negative-feedback loop in vivo. Interestingly, at least three putative sterol regulatory elements and one putative PPARγ binding site are located within −850 bp upstream of the promoter region within the mouse *Crbn* gene. These two transcriptional factors regulate lipogenesis, which may provide mechanistic insights into the nutrient-dependent modulation of *Crbn* expression. Second, it is not clear how AMPK is regulated by Crbn in other organs. The physiological roles of AMPK are established in other organs such as adipose tissue and SKM, but it was not possible to discern the contributions of these organs to the metabolic phenotype in *Crbn* KO mice. The activation of AMPK in WAT and SKM was higher in *Crbn* KO mice than in WT mice (Supplementary Fig. 7). Thus, it is feasible that other organs relative to metabolism may be affected in a way similar to the liver in *Crbn* KO mice.

The liver is regarded as the core center for maintaining glucose homeostasis and lipid metabolism, so understanding the normal physiology and the pathophysiology of hepatic metabolism is a prerequisite to understanding whole-body metabolism (7,9,26). Of a variety of tissues tested, the activity of AMPK is lowest in brain and SKM and highest in the liver (32). This may underlie why deletion of *Crbn*, a negative regulator of AMPK, most affects the liver in *Crbn* KO mice. In addition, alterations in liver function clearly affect whole-body metabolism and underlie the development of metabolic diseases, including type 2 diabetes and metabolic syndromes (7,9). Thus, the current study of the role of Crbn in hepatic metabolism may be the first step toward a greater understanding of the physiological function of *Crbn* at the molecular level during normal and diseased states.

In summary, this study provides the first in vivo evidence that Crbn negatively regulates the activation of AMPK and that *Crbn* deficiency protects mice from obesity, fatty liver, and insulin resistance caused by an HFD. Thus, CRBN may be considered a novel regulator of body metabolism and energy homeostasis.

REFERENCES

1. Higgins JJ, Pucilowska J, Lombardi RQ, Rooney JP. A mutation in a novel ATP-dependent Lon protease gene in a kindred with mild mental retardation. Neurology 2004;63:1927–1931
2. Jo S, Lee KH, Song S, Jung YK, Park CS. Identification and functional characterization of cereblon as a binding protein for large-conductance calcium-activated potassium channel in rat brain. J Neurochem 2005;94:1212–1224
3. Ito T, Ando H, Suzuki T, et al. Identification of a primary target of thalidomide teratogenicity. Science 2010;327:1345–1350
4. Lee KM, Jo S, Kim H, Lee J, Park CS. Functional modulation of AMP-activated protein kinase by cereblon. Biochim Biophys Acta 2011;1813:448–455
5. Hardie DG. AMP-activated/SNF1 protein kinases: conserved guardians of cellular energy. Nat Rev Mol Cell Biol 2007;8:774–785
6. Hawley SA, Davison M, Woods A, et al. Characterization of the AMP-activated protein kinase kinase from rat liver and identification of threonine 172 as the major site at which it phosphorylates AMP-activated protein kinase. J Biol Chem 1996;271:27879–27887
7. Viollet B, Guigas B, Leclerc J, et al. AMP-activated protein kinase in the regulation of hepatic energy metabolism: from physiology to therapeutic perspectives. Acta Physiol (Oxf) 2009;196:81–98
8. Shackelford DB, Shaw RJ. The LKB1-AMPK pathway: metabolism and growth control in tumour suppression. Nat Rev Cancer 2009;9:563–575
9. Viollet B, Foretz M, Guigas B, et al. Activation of AMP-activated protein kinase in the liver: a new strategy for the management of metabolic hepatic disorders. J Physiol 2006;574:41–53

10. Bergeron R, Previs SF, Cline GW, et al. Effect of 5-aminoimidazole-4-carboxamide-1-beta-D-ribofuranoside infusion on in vivo glucose and lipid metabolism in lean and obese Zucker rats. Diabetes 2001;50:1076–1082

11. Hardie DG. AMP-activated protein kinase as a drug target. Annu Rev Pharmacol Toxicol 2007;47:185–210

12. Cool B, Zinker B, Chiou W, et al. Identification and characterization of a small molecule AMPK activator that treats key components of type 2 diabetes and the metabolic syndrome. Cell Metab 2006;3:403–416

13. Dasgupta B, Milbrandt J. Resveratrol stimulates AMP kinase activity in neurons. Proc Natl Acad Sci USA 2007;104:7217–7222

14. Ramamurthy S, Ronnett GV. Developing a head for energy sensing: AMP-activated protein kinase as a multifunctional metabolic sensor in the brain. J Physiol 2006;574:85–93

15. Kelley DE, McKolanis TM, Hegazi RA, Kuller LH, Kalhan SC. Fatty liver in type 2 diabetes mellitus: relation to regional adiposity, fatty acids, and insulin resistance. Am J Physiol Endocrinol Metab 2003;285:E906–E916

16. Kim EJ, Yoon YS, Hong S, et al. Retinoic acid receptor-related orphan receptor α-induced activation of adenosine monophosphate-activated protein kinase results in attenuation of hepatic steatosis. Hepatology 2012; 55:1379–1388

17. Serino M, Menghini R, Fiorentino L, et al. Mice heterozygous for tumor necrosis factor-alpha converting enzyme are protected from obesity-induced insulin resistance and diabetes. Diabetes 2007;56:2541–2546

18. Shimano H. Sterol regulatory element-binding protein-1 as a dominant transcription factor for gene regulation of lipogenic enzymes in the liver. Trends Cardiovasc Med 2000;10:275–278

19. Horton JD, Goldstein JL, Brown MS. SREBPs: activators of the complete program of cholesterol and fatty acid synthesis in the liver. J Clin Invest 2002;109:1125–1131

20. Bocher V, Pineda-Torra I, Fruchart JC, Staels B. PPARs: transcription factors controlling lipid and lipoprotein metabolism. Ann N Y Acad Sci 2002;967:7–18

21. Lehrke M, Lazar MA. The many faces of PPARgamma. Cell 2005;123:993–999

22. Cases S, Smith SJ, Zheng YW, et al. Identification of a gene encoding an acyl CoA:diacylglycerol acyltransferase, a key enzyme in triacylglycerol synthesis. Proc Natl Acad Sci USA 1998;95:13018–13023

23. Niu Y, Li S, Na L, et al. Mangiferin decreases plasma free fatty acids through promoting its catabolism in liver by activation of AMPK. PLoS ONE 2012;7:e30782

24. Vaulont S, Munnich A, Decaux JF, Kahn A. Transcriptional and post-transcriptional regulation of L-type pyruvate kinase gene expression in rat liver. J Biol Chem 1986;261:7621–7625

25. da Silva Xavier G, Leclerc I, Salt IP, et al. Role of AMP-activated protein kinase in the regulation by glucose of islet beta cell gene expression. Proc Natl Acad Sci USA 2000;97:4023–4028

26. Viollet B, Athea Y, Mounier R, et al. AMPK: Lessons from transgenic and knockout animals. Front Biosci 2009;14:19–44

27. Foretz M, Ancellin N, Andreelli F, et al. Short-term overexpression of a constitutively active form of AMP-activated protein kinase in the liver leads to mild hypoglycemia and fatty liver. Diabetes 2005;54:1331–1339

28. Fisher FM, Chui PC, Antonellis PJ, et al. Obesity is a fibroblast growth factor 21 (FGF21)-resistant state. Diabetes 2010;59:2781–2789

29. Fryer LG, Carling D. AMP-activated protein kinase and the metabolic syndrome. Biochem Soc Trans 2005;33:362–366

30. Stapleton D, Mitchelhill KI, Gao G, et al. Mammalian AMP-activated protein kinase subfamily. J Biol Chem 1996;271:611–614

31. Kraja AT, Lawson HA, Arnett DK, et al. Obesity-insulin targeted genes in the 3p26-25 region in human studies and LG/J and SM/J mice. Metabolism 2012;61:1129–1141

32. Davies SP, Carling D, Hardie DG. Tissue distribution of the AMP-activated protein kinase, and lack of activation by cyclic-AMP-dependent protein kinase, studied using a specific and sensitive peptide assay. Eur J Biochem 1989;186:123–128